Vacuum near-field scanning optical microscope for variable cryogenic temperatures

G. Behme, A. Richter, M. Süptitz, and Ch. Lienau[a)]
Max-Born-Institut für Nichtlineare Optik und Kurzzeitspektroskopie, Rudower Chaussee 6, D-12489 Berlin, Germany

(Received 21 May 1997; accepted for publication 24 June 1997)

We describe the design of a novel near-field scanning optical microscope for cryogenic temperatures and operation in vacuum. A helium flow cryostat is used for active temperature control of the sample in the range between 8 and 330 K, while all components of the near-field microscope are kept at room temperature. This design greatly simplifies near-field microscopy at variable sample temperatures and permits large piezoelectric scan ranges of up to $100\times100\times10\ \mu m^3$, the implementation of hardware-linearized piezoelectric scan stages, as well as flexible coarse positioning. First experiments with single GaAs quantum wires demonstrate the excellent performance of this new instrument. © *1997 American Institute of Physics.*
[S0034-6748(97)04809-0]

I. INTRODUCTION

Near-field scanning optical microscopy (NSOM) pushes the resolution of optical microscopy beyond the classic diffraction limit down to below 100 nm. This opens up new and exciting perspectives for using the powerful concepts of optical spectroscopy for the characterization of single nanostructures. Consequently, during the last years, a variety of applications[1,2] of NSOM to, for example, the spectroscopy of single molecules,[3–7] biological samples,[8–10] or semiconductor nanostructures,[11–16] emerged.

An important extension to near-field microscopy is the ability to study the spectroscopic properties of the sample at varying, in particular, cryogenic temperatures. Reasons for performing low-temperature near-field microscopic studies have been discussed in detail by Grober *et al.*[17] Particularly important are the strong increase in the luminescence quantum yield of solids and the suppression of thermally induced line broadening processes at low temperatures. Designs and implementations of low-temperature near-field optical microscopes have been reported by several groups.[17–21] In all these designs the entire microscope setup, consisting of sample holder, near-field (fiber) probe, shear-force tip-to-sample distance control, x-y-z-piezo fine positioning, and coarse positioning, is cooled by either gaseous or liquid helium, depending on the operating temperature. So far, however, there have been rather few applications of these new instruments. This is in part due to several of the following technical difficulties in the implementation of these designs: (i) The scan range of the x-y-z piezos is strongly temperature dependent and decreases at 4 K to about 20% of its room temperature value.[22] This limits the attainable maximum scan range to typically $5\times5\times1\ \mu m^3$ and requires careful scanner calibration for every operation temperature. (ii) Hardware linearization of the piezo nonlinearity is generally not available, which is a problem because of the relatively large scan range needed in NSOM experiments. (iii) Cooldown of the entire microscope setup is necessary and thus thermal equilibration generally occurs on a time scale of several hours.[23] (iv) A change in operation temperature induces a change in temperature and thus in resonance frequency of the shear-force setup generally used for tip-to-sample distance regulation, making experiments at varying sample temperatures difficult.

In this article, we report on the design and operation of a new, variable cryogenic temperature near-field scanning optical microscope that circumvents most of the problems. In this design, the sample is cooled by attaching it to the cold finger of a helium flow cryostat. The cold finger, sample, and NSOM scan head, consisting of a near-field fiber probe, a tuning fork shear-force distance regulation, and coarse and fine positioning, are mounted inside a vacuum chamber. Thus, the sample can be cooled to low temperatures while leaving the temperature of the NSOM scan head uncontrolled and close to room temperature. Such a design opens the possibility for near-field microscopy under ultrahigh vacuum conditions, making it ideal for nanoscopic optical surface science studies.

An outline of the article is as follows. After a description of the microscope design, its mechanical stability and reliability are shown by comparing shear-force topographic images of a calibration grating at different temperatures. The performance of the setup is demonstrated by presenting near-field photoluminescence spectra of a newly developed GaAs quantum wire nanostructure.[24,25]

II. MICROSCOPE DESIGN

The microscope is designed as an insert for a vacuum chamber (Fig. 1) and consists of (i) a continuous flow helium cryostat, (ii) a sample holder, (iii) a near-field fiber probe, (iv) a tuning fork[26] shear-force setup[27,28] to regulate the distance between the near-field probe and the sample surface, (v) piezoelectric actuators for x-y-z fine positioning (on a nanometer scale) of the probe with respect to the sample, (vi) motorized translation stages for x-y-z coarse positioning (on a micrometer scale), and (vii) a microscope objective for far-field imaging of the sample. The microscope is capable

[a)]Author to whom correspondence should be addressed; Electronic mail: lienau@mbi-berlin.de

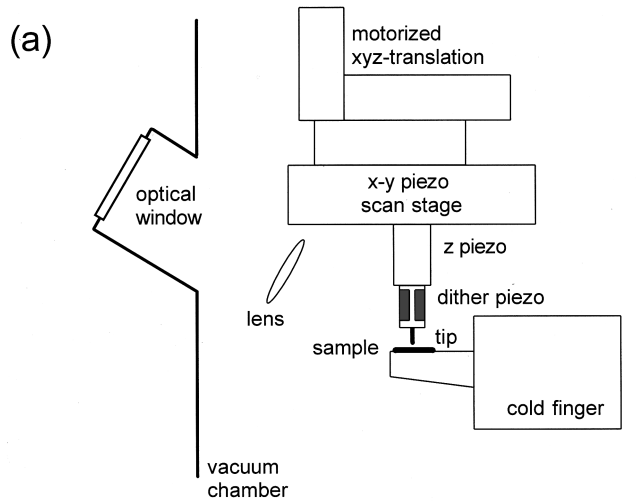

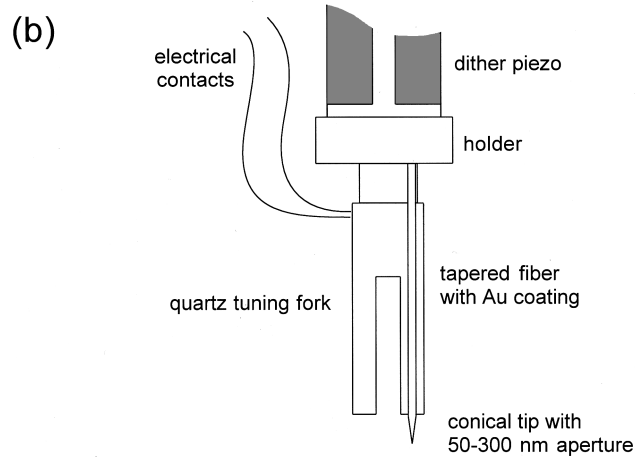

FIG. 1. (a) Schematic diagram of the NSOM scan head. The sample is mounted on a sample holder connected to the cold finger of a continuous flow helium cryostat. The temperature of this cold finger is actively controlled in the range between 8 and 330 K. The NSOM scan head consists of a near-field fiber tip, a tuning fork shear-force tip-to-sample distance regulation, a 10 μm piezoelectric actuator for z motion, a 100 μm$\times$100 μm linearized x-y-piezo scan stage, motorized x-y-z translation stages for coarse positioning and a 0.45 NA microscope objective for far-field illumination or luminescence collection. The entire setup is mounted inside a vacuum chamber. (b) Schematic of the shear-force setup. The near-field fiber probe is rigidly attached to one arm of a quartz tuning fork. A dither piezo is used to excite the tuning fork/tip oscillator to vibrations parallel to the sample surface and the oscillation amplitude is sensed by measuring the piezoelectric potential across the two electrodes of the tuning fork.

of operation in both a reflection or transmission geometry at temperatures between 8 and 330 K. The entire setup is installed on a vibrationally isolated optical table (Newport RS 3000 with I-2000 pneumatic isolators).

The design of the NSOM scan head is shown schematically in Fig. 1(a). The sample is mounted on a gold plated, copper sample holder, connected to the cold finger of a continuous flow liquid helium cryostat (Oxford Instruments, CF 302 M), generally used for low temperature scanning electron microscopy (SEM). The SEM spatial resolution achieved with this a cryostat is better than 20 nm. Temperature regulation of the cold finger is realized with a built-in Rd–Fe temperature sensor and a heater wire. Using an ITC4

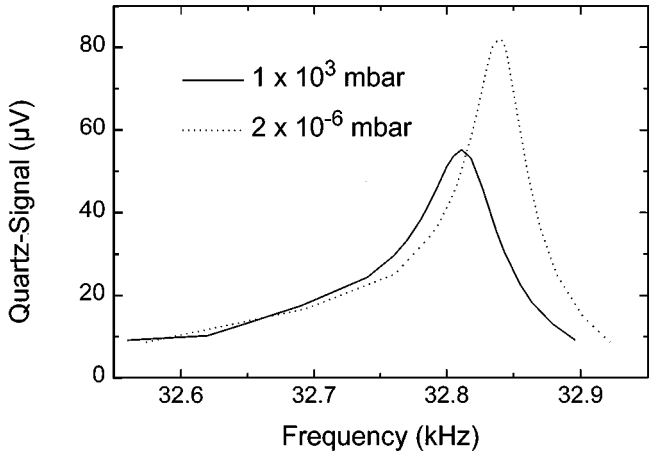

FIG. 2. Amplitude of the tuning fork piezoelectric signal as a function of excitation frequency at pressures of 1 bar (solid line) and 2×10^{-6} mbar (dashed line). The excitation amplitude of the dither piezo is 10 mV. The quality factor of the tuning fork/tip oscillator is about 400 at ambient pressure and increases to 530 at a pressure of 2×10^{-6} mbar.

temperature controller (Oxford Instruments), the temperature stability obtained is better than 0.1 K and the cooldown time is about 30 min.

Near-field probe tips are made by pulling single-mode optical fiber (3M SN 4224) to a sharp taper with a cone angle of 10° in a commercial CO_2-laser based fiber puller (Sutter P 2000) and then coating the taper with a 50–100-nm-thick aluminum or gold layer.[29] Aperture diameters between less than 50 and more than 300 nm at the very end of the taper are obtained by carefully controlling the pulling parameters.[30,31]

The fiber tip is glued along the side of one of the arms of a commercially available quartz crystal tuning fork used as a detector for shear-force distance regulation [Fig. 1(b)]. This tuning fork is attached to a dither piezo tube. The dither piezo tube is used to excite the tuning fork/tip oscillator at its mechanical resonance frequency at about 32 kHz to vibrations parallel to the sample surface by applying an ac voltage of about 10 mV. The tuning fork/tip oscillation amplitude is sensed by measuring the oscillating piezoelectric potential across the two electrodes of the tuning fork using a lock-in voltmeter. The measured voltage is typically on the order of several tens of μV. As the tip approaches the sample surface, the amplitude of the tuning/fork tip oscillation decreases and the corresponding change in lock-in voltage can be used for reliable tip-to-sample distance regulation in the range of 0–20 nm using a feedback loop. As shown in Fig. 2, the quality factor, i.e., the ratio of the full width at half-maximum (FWHM) of the resonance curve (82 Hz) divided by the resonance frequency of the tuning fork/tip oscillator (32.8 kHz) is about 400 at ambient pressure. In vacuum it increases to 530 at a pressure of 2×10^{-6}mbar. For fine positioning of the tip perpendicular to the sample, a low-voltage piezoelectric translator is used, allowing a vertical scan range of 10 μm. In the x-y plane parallel to the sample surface fine positioning is achieved with a hardware-linearized, vacuum compatible x-y monolithic scan stage (Physik Instrumente P 730.20). The maximum scan area of

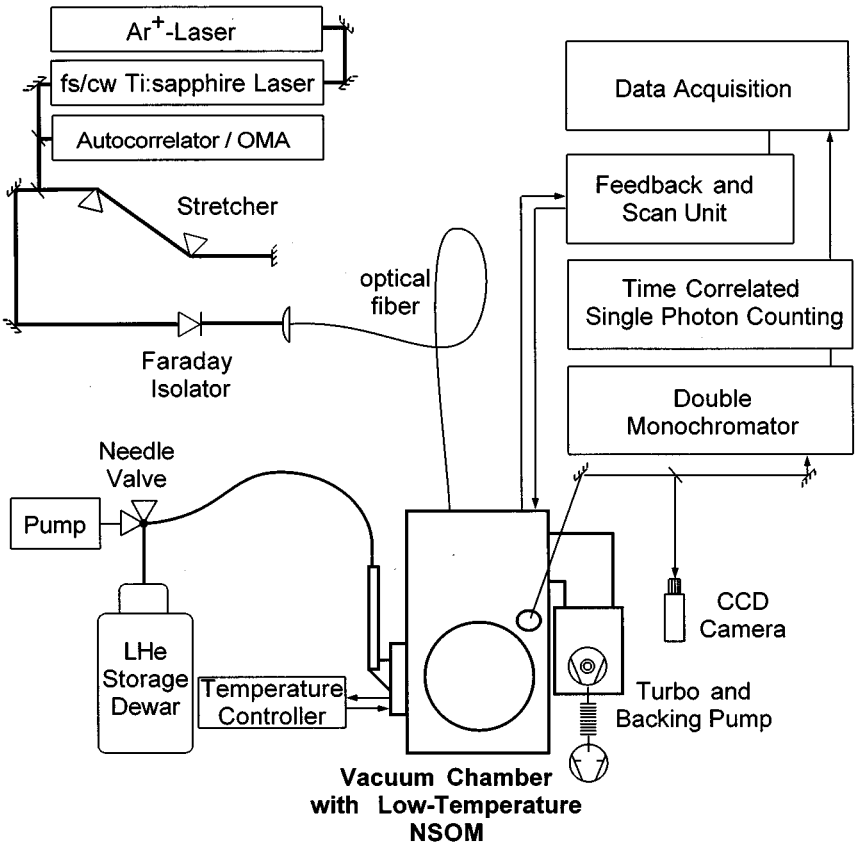

FIG. 3. Block diagram of the NSOM setup. A fs/cw Ti:sapphire laser is used as a tunable excitation light source. The sample and NSOM scan head are mounted inside a vacuum chamber that is evacuated by a magnetic-bearing turbomolecular pump down to a pressure of 2×10^{-7} mbar. In spectroscopic experiments, the sample luminescence is dispersed in a 0.22 m double monochromator and detected with a photon-counting APD diode. Commercially available scanning electronics and software (Topometrix) are used for piezo control and for data acquisition.

the stage is 100×100 μm (at -20 to $+120$ V). Capacitance transducers for on-line position monitoring are included in this stage. The capacitance transducers are parts of positioning servo loops for the x and y axes, respectively (Physik Instrumente).[32] Analog proportional-integral (PI) controllers ensure that the actual scanner position follows the nominal value given by the scan electronics. The repeatability and stability of the position in the x-y plane are mainly limited by mechanical stability and digital-to-analog converter (DAC) noise of the scan electronics. The contribution of the capacitance electronics is only on the order of 1 nm.[32]

Coarse positioning is accomplished by three linear translation stages (Newport UMR) that permit motion in the x, y, and z directions over a range of up to 16 mm. The translation stages are driven by motorized actuators with a minimum step size of 0.5 μm (Newport 860A).

A long working distance (20.5 nm) $20\times$ microscope objective (Nikon SLWD 20) with a 0.4 numerical aperture (NA) mounted inside an adjustable lens holder is attached to the x-y scan stage. It allows visual inspection of the tip–sample region by illuminating it with a light emitting diode (LED), which collects the reflected light through the microscope objective and routes the light onto a charge coupled device (CCD) camera outside the vacuum chamber. This greatly facilitates *in vacuo* tip–sample alignment and in particular coarse positioning of the near-field fiber probe over specific lateral regions of the sample.

The microscope objective moreover also serves for collection of the light reflected (or emitted) by the sample when using the NSOM in illumination mode as well as for far-field illumination of the sample when using the NSOM in collection mode.

A block diagram of our NSOM setup is shown in Fig. 3. The vacuum chamber is evacuated to a pressure of 2×10^{-7} mbar using a magnetic-bearing turbomolecular pump (Seiko STP 300) with a pumping speed of 300 ℓ/s. The mechanical vibrations induced by the pump are small enough to keep the pump running during the NSOM experiments.

In our laboratory, a tunable home-built Ti:sapphire laser pumped by an Ar^+ laser (Coherent Innova) is used for continuous-wave (cw) and short pulse excitation of the sample in the wavelength range between 700 and 900 nm. In time-resolved experiments, compression and spectral shaping of the laser pulses are achieved in a prism based stretcher/compressor unit. In cw experiments, wavelength tuning is achieved by a three-plate birefringent filter inside the laser cavity. In illumination mode experiments, the light is transmitted through a Faraday isolator (Gsänger FR 820 BB) and coupled into the near-field probe using a commercial fiber coupler (Newport). In spectroscopic experiments, the luminescence emitted by the sample is spectrally dispersed in a 0.22 m double monochromator and detected with a (time-correlated) single photon counting system based on a silicon avalanche photodiode detector (ADP, EG&G SPC200

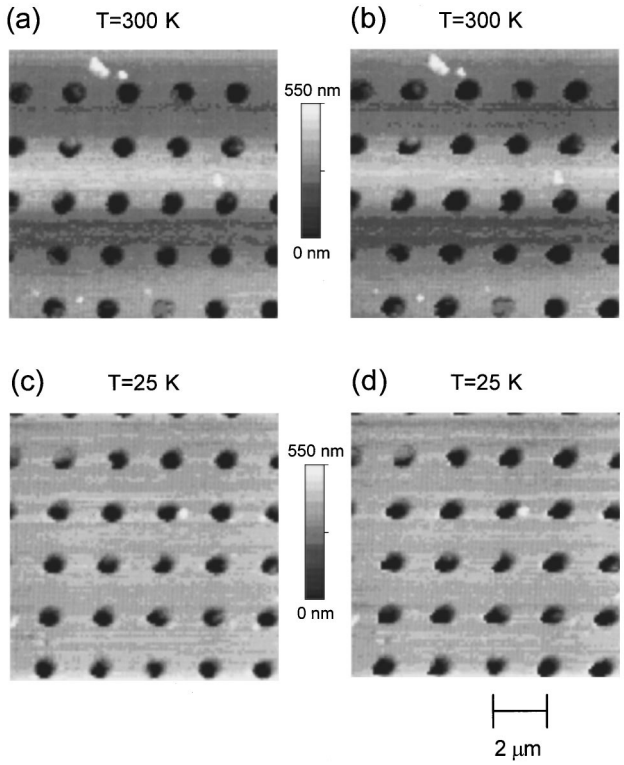

FIG. 4. Shear-force images of the topography of a grating standard (Topometrix). The sample consists of a metal surface with a 2 μm$\times$2 μm grid of equally spaced 400-nm-deep cylindrical pits with an inner diameter of 800 nm. The images are recorded at sample temperatures of 300 K in (a) and (b) and 25 K (c) and (d). Images (a) and (c) are recorded in forward scan direction and (b) and (d) in backward scan direction. All images are taken with uncoated fiber probes at a background pressure of 5×10^{-7}mbar and at a scan speed of 2 μm/s.

CD 2027). Commercially available scanning electronics and software (Topometrix) are used for controlling the piezoelectric x-y stage and for data acquisition.

III. EXPERIMENTAL RESULTS

In order to test the shear-force setup and the mechanical stability of the microscope, shear-force images of the surface topography of a grating standard (Topometrix) were recorded. The sample consists of a metal surface with a 2 μm$\times$2 μm grid of equally spaced 400-nm-deep cylindrical pits with an inner diameter of 800 nm. Figure 4 compares shear-force images recorded at sample temperatures of 300 K [Figs. 4(a) and 4(b)] and 25 K [Figs. 4(c) and 4(d)], with images in (a) and (c) scanned in the forward scan direction and those in (b) and (d) in the backward scan direction. All images were recorded with uncoated fiber probes at a background pressure of 5×10^{-7} mbar and at a scan speed of 2 μm/s. The data clearly demonstrate the stability of the microscope design. The topographic height resolution in these images is better than 10 nm. A comparison of the images taken in the forward and backward scan directions also shows the efficient compensation of x-y scan stage piezo nonlinearity for closed-loop operation of the positioning servo loops.

In near-field experiments, the surface of the cooled sample is in close proximity to the tip of the near-field fiber probe that in our design is not at a controlled temperature. Generally, the tip temperature is significantly higher than the ambient temperature because a significant fraction of the light coupled into the near-field probe is absorbed inside the metal coating at the very end of the fiber probe. In room temperature experiments, this often leads to tip temperatures that are significantly, often more than 100 K, above ambient temperature.[33,34] The near-field fiber probe thus shows a localized heat source directly above the sample area under investigation and its effect on the local sample temperature is *a priori* difficult to estimate. It thus becomes necessary to monitor the local sample temperature directly below the near-field probe. We therefore recorded near-field photoluminescence spectra of newly designed GaAs quantum wire nanostructures using the emission wavelength of these structures as a sensitive probe of the local sample temperature.

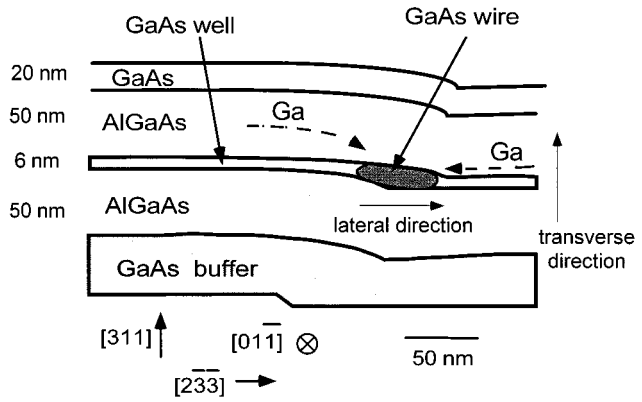

FIG. 5. Schematic of the quantum wire structure (Ref. 24). The sample is grown on patterned GaAs (311)*A* substrates with 15-nm-high mesa stripes oriented along the [01-1] direction. Formation of GaAs quantum wires with a lateral dimension of 50 nm and a vertical dimension of 12 nm is due to the preferential migration of Ga atoms, as indicated by the dashed arrows, during the growth of the 6 nm GaAs quantum well. The GaAs quantum well is sandwiched between two 50 nm AlGaAs layers. The structure is capped with a 20 nm GaAs layer.

In the sample in Fig. 5, an up to 12-nm-thick (z direction) and laterally up to 50-nm-wide (x direction) GaAs quantum wire (QWR) structure is grown by molecular beam epitaxy on patterned GaAs(311) substrates at the sidewall of 15–20-nm-high mesa stripes oriented along [01-1].[24] This quantum wire structure extends over a length of several mm along the y direction and leads to a one-dimensional confinement of the electronic motion along the y-wire axis. In the x-y-plane, the structure is surrounded on both sides by a nominally 6-nm-thick GaAs quantum well (QW). Vertically, the structure is clad by two 50-nm-thick $Al_{0.5}Ga_{0.5}As$ barriers. The sample surface is covered by a 20-nm-thick GaAs cap layer so that the quantum wire structure is located approximately 75 nm below the sample surface.

In microphotoluminescence (μ-PL) experiments recorded in a conventional confocal spectrometer, the photoluminescence emission of the QWR and the embedded QW are energetically well separated. At a sample temperature of 8 K, the QWR emission peak is centered at 1.544 eV and has a FWHM of 8.5 meV, whereas the QW emission peaks at 1.602 eV (FWHM 13 meV). Increasing the sample temperature to 100 K leads to a shift of the two peaks to 1.535 and

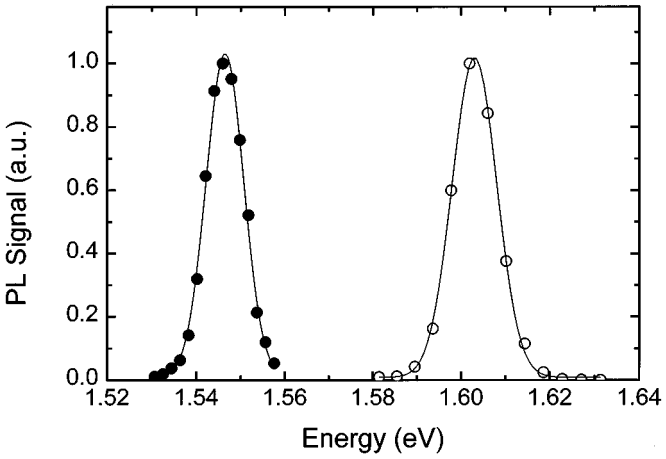

FIG. 6. Near-field photoluminescence spectra of the sidewall GaAs quantum wire (closed circles) and the embedding 6 nm GaAs quantum well (open circles). The nominal sample temperature is 8 K. The spectra are recorded for spatially resolved illumination of the sample by transmitting light at a photon energy of 1.959 eV through the 150 nm aperture of a near-field fiber probe. Luminescence is collected using a far-field microscope objective.

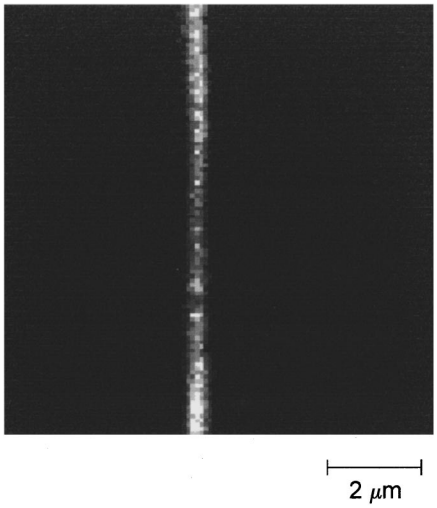

FIG. 7. Quantum wire luminescence for spatially resolved resonant QWR excitation at an energy of 1.57 eV. The excitation light is transmitted through the 250-nm-diam aperture of the near-field probe and the far-field QWR luminescence is detected at an energy of 1.543 eV. The nominal sample temperature is 8 K. The QWR axis is oriented along the *y* direction while, along the *x* direction, the near-field probe is scanned perpendicular to the wire axis. The scan range in this image is 9 μm×9 μm and the image was recorded at a scan rate of 2 μm/s.

1.595 eV, respectively. These μ-PL spectra are now compared to spectra recorded in our near-field setup in an illumination mode geometry. Spatially resolved optical excitation of the sample was achieved by transmitting the excitation light at 1.959 eV through the aperture at the end of the NSOM probe tip. The aperture size in these experiments was about 150 nm. Photoluminescence emitted by the sample was then collected through the microscope objective in reflection geometry. The PL was dispersed in the 0.22 m double monochromator and detected with the Si avalanche photodiode in a single photon counting mode. The nominal sample temperature, measured with the temperature sensor built into the cold finger of the cryostat, was 8.0 ± 0.1 K. No increase in sample temperature was detected with this sensor after bringing the near-field fiber probe into feedback. As shown in Fig. 6, the near-field PL spectrum of the QWR structure shows a single narrow peak at 1.546 eV with a width of 8 meV (FWHM), whereas in the QW spectrum it is centered at 1.603 eV (FWHM 13 meV). These spectra, which reflect the **local** sample temperature directly below the near-field probe, give no indication of a significant increase in sample temperature due to the presence of the near-field probe. These results together with the results of a variety of spectroscopic experiments at different sample temperatures that are reported elsewhere indicate that it is safe to assume that the local sample temperature in the presence of the near-field tip is well below 20 K.

Resonant excitation of the sample at an energy of 1.57 eV, i.e., below the QW band gap, allows us to excite **only** the QWR structure. In a spatially resolved experiment, QWR excitation thus becomes possible only if the near-field probe is located in the direct vicinity of the QWR. Figure 7 presents a two-dimensional illumination mode scan of the QWR emission at a fixed detection energy of 1.543 eV for excitation at 1.57 eV at a sample temperature of 8 K. The QWR axis is oriented along the *y* direction while, along the *x* direction, the near-field probe is scanned perpendicular to the wire axis. The scan range in this image is 9 μm×9 μm and the image was recorded at a scan rate of 2 μm/s. To obtain a good signal-to-noise ratio in a single scan, a rather large (250 nm) aperture of the near-field probe was chosen in this experiment.

The experiment directly shows that QWR emission is only observed for a direct overlap of the electromagnetic near-field distribution inside the sample and the QWR structure. It clearly demonstrates (i) the high mechanical stability of our setup and (ii) the sensitivity and reliability of the entire NSOM setup.

The spatial resolution in this experiment is limited to considerably below 400 nm and is given by the convolution of the finite aperture size and the finite intrinsic resolution that is achievable for this sample, which is also on the order of 250 nm. This intrinsic resolution is limited by the specific layer structure of the sample—in particular by the 75 nm distance between the QWR structure and the high refractive index of about 3.5 of the sample which causes a rapid broadening of the near-field distribution inside the sample.[16] Significantly increased spatial resolution is expected for QWR structures located closer to the sample surface and experiments are currently underway to verify this.

The experimental results presented are part of a complete spectroscopic study of nanoscopic optical studies of this GaAs heterostructure. Spatially resolved near-field photoluminescence and photoluminescence excitation spectra at varying temperatures will be discussed in a future publication.[35] These spectra give detailed and direct information on (i) local, growth correlated variations of the band gap potential in this semiconductor nanostructure on a subwavelength length scale, and (ii) carrier exchange processes between systems of different dimensionality, i.e., the one-dimensional quantum wire and the embedded two-

dimensional quantum well, and their particular sensitivity to the details of the **local** bandstructure.

In summary, we have discussed the design of a new, variable cryogenic temperature near-field scanning optical microscope. The instrument uses a helium flow cryostat for active temperature control of the sample in the range between 8 and 330 K, while the temperature of the NSOM scan head is close to ambient temperature. This design combines large piezoelectric scan ranges of up to $100\times100\times10$ μm^3, the implementation of hardware-linearized piezoelectric scan stages, flexible coarse positioning, and rapid cooldown time with the ability of rapid and greatly simplified sample temperature variation. It demonstrates a new approach to superresolution optical surface spectroscopy in an ultrahigh vacuum environment.

Spectroscopic experiments on a new GaAs quantum wire heterostructure demonstrate the potential of this new instrument, particularly for luminescence spectroscopy or mesoscopic semiconductor systems.

[1] For a recent overview, see, Proceedings of the 4th International Conference on Near-Field Optics, Brunn, 1995; Ultramicroscopy **61** (1995).
[2] M. A. Paesler and P. Moyer, *Near-Field Optics: Theory, Instrumentation and Applications* (Wiley, New York, 1996).
[3] R. X. Bian, R. C. Dunn, X. S. Xie, and P. T. Leung, Phys. Rev. Lett. **75**, 4772 (1995).
[4] E. Betzig and R. J. Chichester, Science **262**, 1422 (1993).
[5] X. S. Xie and R. C. Dunn, Science **265**, 361 (1994).
[6] W. P. Ambrose, P. M. Goodwin, J. C. Martin, and R. A. Keller, Science **265**, 364 (1994).
[7] W. E. Moerner, T. Plakthotnik, T. Irngartinger, U. P. Wild, D. W. Pohl, and B. Hecht, Phys. Rev. Lett. **73**, 2764 (1994).
[8] J. W. Blatchford, T. L. Gustafson, A. J. Epstein, D. A. V. Bout, J. Kerimo, D. A. Higgins, P. F. Barbara, D.-K. Fu, T. M. Swager, and A. G. MacDiarmid, Phys. Rev. B **54**, R3683 (1996).
[9] J. Hwang, L. K. Tamm, C. Bohm, T. S. Ramalingam, E. Betzig, and M. Edidin, Science **270**, 610 (1995).
[10] R. C. Dunn, E. V. Allen, S. A. Joyce, G. A. Anderson, and X. S. Xie, Ultramicroscopy **57**, 113 (1995).
[11] H. F. Hess, E. Betzig, T. D. Harris, L. N. Pfeiffer, and K. W. West, Science **264**, 1740 (1994).
[12] T. D. Harris, D. Gershoni, R. D. Grober, L. Pfeiffer, K. West, and N. Chand, Appl. Phys. Lett. **68**, 988 (1996).
[13] J. Levy, V. Nikitin, J. M. Kikkawa, A. Cohen, N. Samarth, R. Garcia, and D. D. Awschalom, Phys. Rev. Lett. **76**, 1948 (1996).
[14] F. Flack, N. Samarth, V. Nikitin, P. A. Crowell, J. Shi, J. Levy, and D. D. Awschalom, Phys. Rev. B **54**, 17 312 (1996).
[15] M. J. Gregor, P. G. Blome, R. G. Ulbrich, P. Grossmann, S. Grosse, J. Feldmann, W. Stolz, E. O. Gobel, D. J. Arent, and M. Bode, Appl. Phys. Lett. **67**, 3572 (1995).
[16] A. Richter, M. Süptitz, Ch. Lienau, T. Elsaesser, M. Ramsteiner, R. Notzel, and K. H. Ploog, Surf. Interface Anal. **25**, 583 (1997).
[17] R. D. Grober, T. D. Harris, J. K. Trautman, and E. Betzig, Rev. Sci. Instrum. **65**, 626 (1994).
[18] M. J. Gregor, S. Grosse, P. G. Blome, and R. G. Ulbrich, Photons and Local Probes, Proceedings of the NATO Advanced Research Workshop, Reichenau, Germany, 1994, p. 133.
[19] H. Ghaemi, C. Gates, and B. B. Goldberg, Ultramicroscopy **57**, 165 (1995).
[20] J. Levy, V. Nikitin, J. M. Kikkawa, D. D. Awschalom, and N. Samarth, J. Appl. Phys. **79**, 6095 (1996).
[21] A. Deisenrieder, C. Obermüller, K. Karrai, W. Wegscheider, M. Biechler, and G. Abstreiter, in Ref. 1, Book of Abstracts.
[22] R. David, K. Kern, P. Zeppenfeld, and G. Comsa, Rev. Sci. Instrum. **57**, 2771 (1986).
[23] A. R. Smith and C. K. Shih, Rev. Sci. Instrum. **66**, 2499 (1995).
[24] R. Nötzel, M. Ramsteiner, J. Menniger, A. Trampert, H.-P. Schönherr, L. Däweritz, and K. H. Ploog, Jpn. J. Appl. Phys., Part 2 **35**, L297 (1996).
[25] R. Nötzel, J. Menniger, M. Ramsteiner, A. Ruiz, H.-P. Schönherr, and K. H. Ploog, Appl. Phys. Lett. **68**, 1132 (1996).
[26] K. Karrai and R. D. Grober, Appl. Phys. Lett. **66**, 1842 (1995).
[27] E. Betzig, P. L. Finn, and J. S. Weiner, Appl. Phys. Lett. **60**, 2484 (1992).
[28] P. C. Yang, Y. Chen, and M. Vaez-Irvani, J. Appl. Phys. **71**, 2499 (1992).
[29] E. Betzig, J. K. Trautman, T. D. Harris, J. S. Weiner, and R. L. Kostelak, Science **251**, 1468 (1991).
[30] S. Madsen, N. C. R. Jolme, P. S. Ramanujam, S. Hvilsted, J. M. Hvam, and S. Smith (unpublished).
[31] G. A. Valoskovic, M. Holton, and G. H. Morrison, Appl. Opt. **34**, 1215 (1995).
[32] O. Jusko, X. Zhao, H. Wolff, and G. Wilkening, Rev. Sci. Instrum. **65**, 2514 (1994).
[33] M. Stahelin, M. A. Bopp, G. Tarrach, A. J. Meixner, and I. Zschokkegranacher, Appl. Phys. Lett. **68**, 2603 (1996).
[34] Ch. Lienau, A. Richter, and T. Elsaesser, Appl. Phys. Lett. **69**, 325 (1996).
[35] A. Richter, G. Behme, M. Süptitz, Ch. Lienau, T. Elsaesser, R. Nötzel, M. Ramsteiner, and K. H. Ploog (unpublished).